

**Electronic Supplementary Information (ESI) for Soft Matter**

# **Electronic Supplementary Information (ESI)**

## **UV Patternable Thin Film Chemistry for Shape and Functionally Versatile Self-Oscillating Gels**

Peixi Yuan<sup>a</sup>, Olga Kuksenok<sup>b</sup>, Dustin E. Gross<sup>a</sup>, Anna C. Balazs<sup>b</sup> and Jeffery S. Moore<sup>a</sup>, Ralph G. Nuzzo<sup>a,\*</sup>

<sup>a</sup> *School of Chemical Sciences, University of Illinois-Urbana Champaign, Urbana, Illinois 61801*

<sup>b</sup> *Chemical Engineering Department, University of Pittsburgh, Pittsburgh, Pennsylvania 15261*

\*Corresponding author: (tel) 1-217-244-0809; (fax) 1-217-244-2278;  
email: r-nuzzo@illinois.edu

## 1. Characterization of Compound 1, 2 and 3.

### 1.1 NMR characterizations and Mass Spectrometry of 4-hydroxymethyl-4'-methylbpy (1)

<sup>1</sup>H NMR (CDCl<sub>3</sub>, 400 MHz): δ 8.59 (d, J = 4.8 Hz, 1H), 8.50 (d, J = 5.2 Hz, 1H), 8.31 (s, 1H), 8.19 (s, 1H), 7.28 (dd, J = 4.8 Hz, J = 0.8 Hz, 1H), 7.13 (d, J = 5.2 Hz, 1H), 4.77 (d, J = 2 Hz, 2H, CH<sub>2</sub>), 3.46 (bs, 1H, OH), 2.43 (s, 3H, CH<sub>3</sub>)

<sup>13</sup>C NMR (CDCl<sub>3</sub>, 100 MHz): δ 156.0, 155.8, 151.5, 149.1, 148.7, 148.4, 124.8, 122.2, 121.1, 118.6, 63.2(CH<sub>2</sub>), 21.1(CH<sub>3</sub>);

HRMS (ESI +) calculated for C<sub>12</sub>H<sub>13</sub>N<sub>2</sub>O: m/z = 201.1031, found m/z = 201.1028.

### 1.2. NMR characterizations and Mass Spectrometry of [Ru(II)(2,2'-bpy)<sub>2</sub>(4-hydroxymethyl-4'-methylbpy)](PF<sub>6</sub><sup>-</sup>)<sub>2</sub>(2)

<sup>1</sup>H NMR (DMSO-d<sub>6</sub>, 500 MHz): δ 8.82 (d, J = 8.0 Hz, 4H, ArH), 8.71 (d, J = 11.0 Hz, 2H, ArH), 8.15 (t, J = 8.0 Hz, 4H, ArH), 7.73 (t, J = 5.5 Hz, 4H, ArH), 7.64 (d, J = 5.5 Hz, 1H, ArH), 7.52 (m, 5H, ArH), 7.45 (d, J = 5.5 Hz, 1H, ArH), 7.36 (d, J = 6.0 Hz, 1H, ArH), 5.71 (t, J = 5.5 Hz, 1H, OH), 4.73 (d, J = 6.0 Hz, 2H, CH<sub>2</sub>), 2.52 (s, 3H, CH<sub>3</sub>);

<sup>13</sup>C NMR (DMSO-d<sub>6</sub>, 125 MHz): 156.5, 156.0, 154.1, 151.1, 151.0, 150.6, 150.2, 149.8, 137.6, 128.5, 127.7, 125.0, 124.9, 124.3, 121.3, 61.2, 20.5.

HRMS (ESI +) calculated for C<sub>32</sub>H<sub>28</sub>N<sub>6</sub>OF<sub>6</sub>PRu (M<sup>2+</sup>): m/z = 759.1008, found m/z = 759.1010.

### 1.3. Characterizations of Ru(bpy)<sub>2</sub>(4-methacryloylmethyl-4'-methylbpy)<sub>2</sub><sup>+</sup>(PF<sub>6</sub><sup>-</sup>)<sub>2</sub> (3)

As shown in S. Fig.1, <sup>1</sup>H NMR (DMSO-d<sub>6</sub>, 500 MHz,): δ 8.83 (m, 5H, ArH), 8.71 (s, 1H, ArH), 8.15 (t, J = 8.0 Hz, 4H, ArH), 7.74-7.70 (m, 5H, ArH), 7.56-7.49 (m, 6H, ArH), 7.38 (d, J = 6.0 Hz, 1H, ArH), 6.17 (t, J = 1.5 Hz, 1H, C=CH), 5.79 (t, J = 1.5 Hz, 1H, C=CH), 5.39 (s, 2H, CH<sub>2</sub>), 2.52 (s, 3H, bpy-CH<sub>3</sub>), 1.93 (s, 3H, C=CCH<sub>3</sub>);

As shown in S. Fig.2, <sup>13</sup>C NMR (DMSO-d<sub>6</sub>, 125 MHz,): 166.2 156.60, 156.57, 156.5, 155.8, 151.4, 151.2, 150.4, 149.9, 147.5, 137.9, 135.3, 128.9, 127.9, 127.2, 125.3, 124.5, 122.3, 63.7(pyr-CH<sub>2</sub>), 20.8(pyr-CH<sub>3</sub>), 18.0(CH<sub>3</sub>)

As shown in S. Fig. 3, HRMS (ESI +) calculated for C<sub>36</sub>H<sub>32</sub>N<sub>6</sub>O<sub>2</sub>F<sub>6</sub>PRu (M<sup>2+</sup>): m/z = 827.1281, found m/z = 827.1272.

## 2. Fabrication of 110μm Thick BZ-Gel.

The prepolymer mixture is the same as described in section 2.3. 2mL pregel monomer mixture solutions were evenly spread on a 2-inch diameter silicon wafer. The sample was exposed under a mask aligner, with a 298 nm UV light source, at 300 watt power (exposure dose=8mJ/cm<sup>2</sup>) for 150 seconds. The wafer was then gently immersed in D.I. water overnight to remove excess monomer and photoinitiator. Meanwhile, the gels would be delaminated from the wafer and ready for application. The gel fabricated this way has a thickness around 110 μm (S. Fig. 6a).

## 3. Swell-Deswell Properties of PAAm Based BZ Gels

The size and strained change of the PAAm based BZ-gels in fully oxidized and reduced state were investigated. The circular shaped gel (S.Fig. 7a) has a diameter of 2.14 mm at reduced state, and 1.97 mm at oxidized state, with a strain of 7.94%. In triangular shaped gel (S.Fig. 7b), the side length is 2.28mm at reduced state and 2.01 mm at oxidized state, with a strain of 11.8%. The square shaped gel (S.Fig. 7c) has an edge length of 2.08 mm at reduced state and 1.84 mm at the oxidized state, with a strain of 11.53%. The star shaped gel (S.Fig. 7d) has a distance of 2.32mm at reduced state and 2.08 mm at oxidized state in between 2 convex vertices, yield a strain of 10.3%. The results show PAAm based gels are larger in physical dimensions at reduced state than the oxidized states.

#### 4. Modulus Studies of the PAAm Based BZ-Gel

The polymer with 20 mg crosslinker in the network was chosen as the example for the test of modulus by Atomic Force Microscope (AFM)<sup>1</sup>. Sample was characterized with a silicon nitride cantilever with a spring constant of 0.215 N/m (Veeco) using an MFP 3D AFM (Asylum Research). A conical tip approximation for the AFM tip of Hertz model was used<sup>2</sup>:

$$F = \frac{2}{\pi} \frac{E\delta^2}{(1-\nu^2)} \tan(\alpha) \quad (1)$$

Where F is the loading force from the AFM cantilever, E is the Young's modulus of the self-oscillating gel,  $\delta$  is the depth in the surface of the sample that is caused by the loading force,  $\nu$  is the Poisson ratio (assumed as 0.5<sup>3</sup>), and  $\alpha$  is the half opening angle (18°) of the cantilever. The force diagram of the sample is shown in S. Fig. 8.

Meanwhile, the force F can also be determined by Hooke's law.

$$F = kd = k(z - \delta) \quad (2)$$

Where d is the cantilever deflection and z is the height of the piezo. Combining equations 1 and 2 results in:

$$z - z_0 = d - d_0 + \sqrt{\frac{k(d - d_0)}{(2/\pi)[E/(1-\nu^2)]\tan\alpha}} \quad (3)$$

A thermal power spectral density (PSD) graph was fit to a simple harmonic oscillator function for each individual cantilever to calculate the spring constant k. Individual force curves were modeled with equation 3 using a least squares fit by adjusting E. S. Fig. 8 shows, the typical force curve on the particle with 20 mg (5.76% m/m) corsslinker. And the modulus of the PAAm based BZ gel is 427.6 kPa.

## 5. Computational modeling of PAAm based BZ gels

Herein, we modified our recently developed three-dimensional gel Lattice Spring Model (gLSTM)<sup>4</sup> to capture the chemo-responsive dynamics of PAAm based BZ gels. Our gLSTM approach utilizes a modified Oregonator model for the BZ reaction in solution<sup>5, 6</sup> and incorporates equations for the elastodynamics of the chemo-responsive polymer network. The Oregonator model describes the kinetics of the BZ reaction in terms of the dimensionless concentrations of the oxidized catalyst,  $v$ , and the key reaction intermediate (the activator),  $u$ . With our modifications of the Oregonator model, all the reaction equations now explicitly depend on the volume fraction of polymer,  $\phi$ . The resulting dynamical equations and details of the numerical approach in three dimensions can be found in Ref.<sup>4</sup>. To study the effects of varying the concentration of the Ru catalyst, we further modified the reaction kinetics terms by

utilizing an approach developed in Ref. <sup>7</sup>; the latter approach is based on an improved Oregonator model that explicitly accounts for the total concentration of the Ru catalyst in the governing equations <sup>8</sup>. Recently, we used the same approach to examine the effects of the total Ru concentration on both the period and amplitude of oscillations of PNIPAAm based BZ gels <sup>9</sup>. Modified equations for the reaction kinetics in BZ gels using this improved Oregonator model are provided in eqs. 4.8 and 4.9 of Ref. <sup>10</sup>.

As we described in the text above, the oxidation of the Ru catalyst leads to contraction of the PAAm gel; we assumed that this contraction is due to formation of additional reversible crosslinks when the Ru catalyst is in the oxidized state (see schematic in Fig. 9a). We accounted for this mechanism by dynamically modifying the crosslink density,  $c_0$ , which depends on the concentration of the oxidized catalyst,  $v$ , as  $c_0 = c_0^{BIS} + \tilde{c}_0(v)$ , where  $c_0^{BIS}$  is the density of the permanent crosslinks, and  $\tilde{c}_0(v) = b \cdot v$  denotes the density of the additional reversible crosslinks created by the oxidized Ru catalyst. These crosslinks are broken when all the catalyst is in the reduced state, i.e., when  $v = 0$ . We treated the value of  $b$  as a fitting parameter of the model. (In general,  $b$  could depend on a number of parameters, such as the efficiency of forming additional crosslinks, which in turn, depends on the crosslink density; here, for simplicity we neglect these effects.) Hence, in our model the strength of chemomechanical coupling in PAAm BZ gels is defined by the fitting parameter  $b$ , which accounts for the formation of additional crosslinks upon catalyst oxidation. (This is distinctly different from the chemomechanical coupling in PNIPAAm gels where the oxidized catalyst has a hydrating effect on the polymer network and is accounted for through the parameter  $\chi^*$  <sup>4, 6, 9</sup> that describes the interaction between the oxidized catalyst and the solvent within the framework of the Flory-Huggins theory; here, we set  $\chi^* = 0$

in our gLSM formulation. [NOTE: Interestingly, for a fixed crosslink density, we were able to reproduce pattern formation similar to patterns shown in simulations in Fig.4 by setting a phenomenological parameter describing mechano-chemical coupling to have negative values,  $\chi^* < 0$ , and setting  $b = 0$ . Additional simulations, however, showed that without accounting for the formation of additional reversible crosslinks, it is not possible to reproduce the decrease in amplitude of oscillations in the sample size with the increase in the sample's cross-link density observed experimentally and reported in Fig. 11. The distinction between these two modeling approaches strongly supports the hypothesis that formation of additional crosslinks upon catalyst oxidation is responsible for the observed shrinking of the sample and has to be accounted for in the model explicitly. (i.e., by setting  $b > 0$  in the approach presented here).] ]

We chose our simulation parameters based on the available experimental data. We used the same notation for all our model parameters as provided in Refs. <sup>4</sup> (see also eqs. 4.8 and 4.9 in Ref <sup>10</sup> describing the modified reaction kinetics). For the volume fraction of the polymer in the undeformed state, we set  $\phi_0 = 0.13$ , which corresponds to the fraction of PAAm used in preparation of the gel in experiments herein (see section 2.3 in the text). For the Flory-Huggins parameter describing the polymer-solvent interaction, we set  $\chi_0 = 0.48$  (see Refs. <sup>11, 12</sup>). Note that for the PAAm gels, the Flory-Huggins interaction parameter is assumed to be independent of the polymer volume fraction,  $\phi$  <sup>11, 12</sup>; hence, we set  $\chi_1 = 0$  in our gLSM formulation<sup>4</sup>. The dimensionless crosslink density formed by the permanent MBAAm crosslinks,  $c_0^{BIS}$ , is proportional to the crosslinker concentration and to the efficiency of forming these crosslinks. To ensure that our chosen parameters correspond closely to the experimental system herein, we calculated the equilibrium degree of swelling,  $\lambda_{eq} = (\phi_0 / \phi_{eq})^{1/3}$ , where  $\phi_{eq}$  is the volume fraction

of polymer at equilibrium, as a function of the dimensionless crosslink density,  $c_0^{BIS}$  (see Fig. S9). We found that a reasonably good agreement with the experimental data can be achieved if we assume a relatively low efficiency of forming permanent crosslinks (i.e., that roughly about 5% of the available crosslinker participates in the formation of permanent crosslinks). Such low crosslink efficiency is in agreement with the prior experimental findings on PAAm gel<sup>12,13</sup>.

In Fig. S9, the solid line  $\lambda_{eq}(c_0^{BIS})$  represents the analytical solution that results from equating the elastic and the osmotic pressures<sup>4</sup> in the gel and using the above parameters. Notably, the data obtained from the computer simulations on small samples with all the catalyst being in the reduced state (and no BZ reaction) exactly overlaps this line, showing excellent agreement between the simulations and analytical calculation. The experimental points (red squares) on this plot were obtained by measuring the linear size of the sample in pure water, with the marked values of the weight of the MBAAm crosslinker added to 160 mg of PAAm and 1mL of solvent (see section 2.3 in the text). Hence, the reference value of the dimensionless crosslink density we used in our simulations,  $c_0^{BIS} = 1.25 \times 10^{-4}$ , corresponds to 10mg of MBAAm crosslinker used in these experiments.

We set the values of the reaction parameters in our reference case to correspond to the concentrations of chemical reagents that were used to obtain the experimental data marked by the squares in Figs.11a-b. Namely, the following concentrations were used in the experiments: malonic acid,  $[MA]=0.20M$ , sodium bromate,  $[NaBrO_3]=0.20M$ , and nitric acid  $[HNO_3]=0.30M$ ; based on these values, we set our corresponding simulation parameters (see Ref.<sup>6</sup> for definitions) to  $B=0.2M$ ,  $A=0.2M$  and  $H=0.3M$ . With these values, we estimated that  $\varepsilon=0.15$  in the Oregonator model and calculate the scaling parameter between our simulations and the

experimental concentration of Ru catalyst to be  $Z_0 = 5.6\text{mM}$  (here, we use the same reaction constants for the main processes in the BZ reaction as listed in Ref.<sup>6</sup>). The dimensionless concentration of Ru catalyst,  $c_{Ru}$ , is calculated as  $c_{Ru} = C_{Ru} / Z_0$  where  $C_{Ru}$  is the corresponding experimental value. The reference value of the dimensionless concentration of Ru catalyst we use in our simulations is  $c_{Ru} = 1.5$  (unless specified otherwise); this value corresponds to 8 mg of Ru catalyst used during the gel preparation, as specified in the section 2.3 above. Based on the above scaling, the maximum density of additional crosslinks for the given concentration of Ru catalyst should not exceed  $\tilde{c}_{\max} = 3.6 \times 10^{-4}$ .

For the remaining parameters for the improved Oregonator model, we set the following values<sup>7</sup>:  $\xi = 1$ ,  $\mu = 90$ ,  $q = 9.52 \times 10^{-5}$ , and  $f = 0.9$ . Finally, for our model parameter describing the chemomechanical coupling in our system, we set  $b = 9.5 \times 10^{-4}$ ; with this value, the maximum density of additional crosslinks is  $\tilde{c}_{\max} = 3.1 \times 10^{-4}$  (i.e., it is lower than the upper limit for the given Ru concentration defined above). The remaining gLSM parameters that were not listed above are taken to be the same as in Ref.<sup>4</sup>. With the above parameter values, the dimensionless units of time and length in our simulations can be estimated as  $T_0 \sim 0.4\text{s}$  and  $L_0 \sim 0.02\text{mm}$ , respectively. Hence, the gel sizes used in the above simulations corresponded to the following values. The sample sizes in Fig. 4a-b are  $50 \times 50 \times 6$  and  $90 \times 22 \times 6$  nodes, respectively, corresponding to the dimensions of  $1.37 \times 1.37 \times 0.14\text{ mm}$  and  $2.49 \times 0.59 \times 0.14\text{ mm}$ . The sample size used in Figs.10-11 is  $6 \times 6 \times 2$  nodes, which approximately corresponds to  $0.14 \times 0.14 \times 0.03\text{ mm}$ .

## References

1. R. Dong, T. W. Jensen, K. Engberg, R. G. Nuzzo and D. E. Leckband, *Langmuir*, 2007, **23**, 1483-1488.
2. J. Domke and M. Radmacher, *Langmuir*, 1998, **14**, 3320-3325.
3. T. R. Matzelle, G. Geuskens and N. Kruse, *Macromolecules*, 2003, **36**, 2926-2931.
4. O. Kuksenok, V. V. Yashin and A. C. Balazs, *Physical Review E*, 2008, **78**, 041406.
5. V. V. Yashin and A. C. Balazs, *Science*, 2006, **314**, 798-801.
6. V. V. Yashin and A. C. Balazs, *J. Chem. Phys.*, 2007, **126**, 124707.
7. V. V. Yashin, O. Kuksenok and A. C. Balazs, *J. Phys. Chem. B*, 2010, **114**, 6316-6322.
8. T. Amemiya, T. Yamamoto, T. Ohmori and T. Yamaguchi, *J. Phys. Chem. A*, 2002, **106**, 612-620.
9. I. C. Chen, O. Kuksenok, V. V. Yashin, R. M. Moslin, A. C. Balazs and K. J. Van Vliet, *Soft Matter*, 2011, **7**, 3141-3146.
10. V. V. Yashin, O. Kuksenok, P. Dayal and A. C. Balazs, *Rep Prog Phys*, 2012, **75**.
11. J. P. Baker, L. H. Hong, H. W. Blanch and J. M. Prausnitz, *Macromolecules*, 1994, **27**, 1446-1454.
12. M. Y. Kizilay and O. Okay, *Polymer*, 2003, **44**, 5239-5250.
13. S. Durmaz and O. Okay, *Polymer*, 2000, **41**, 5729-5735.

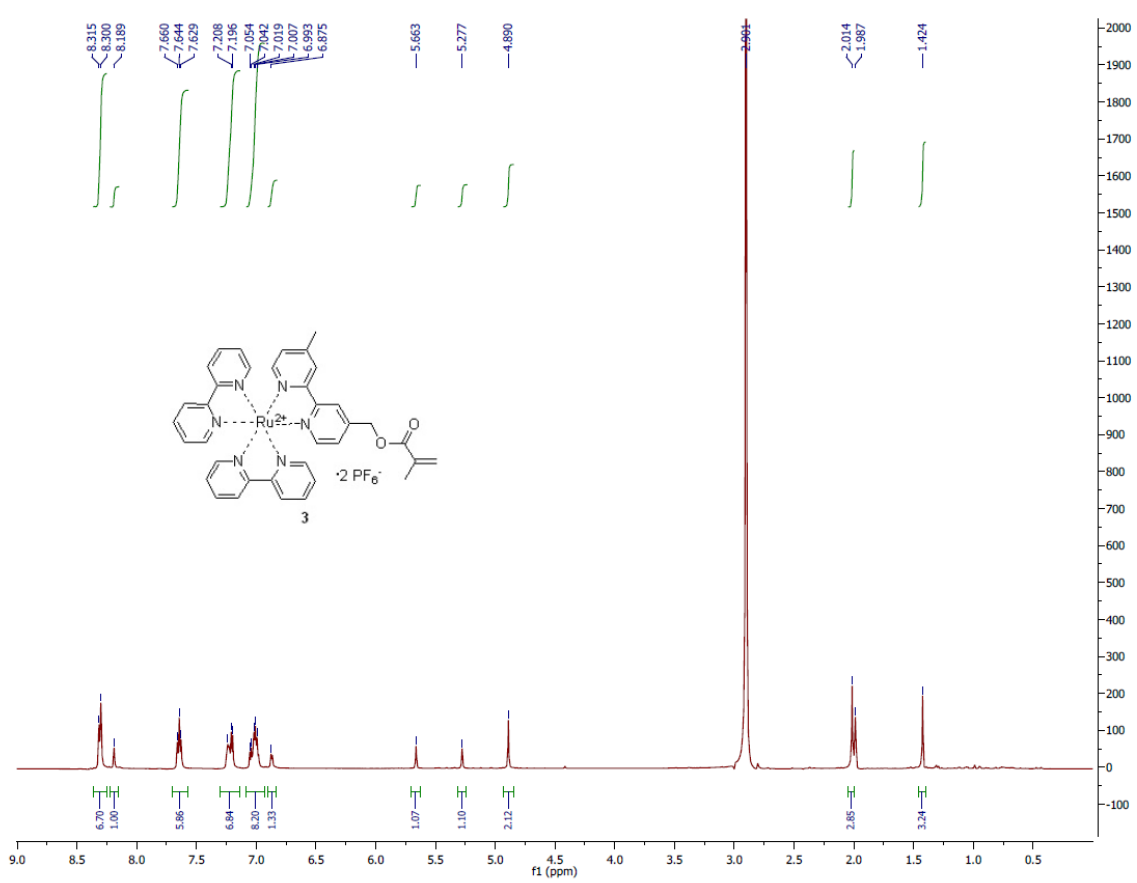


**Figure S1:**  $^1\text{H}$  NMR spectroscopy for  $[\text{Ru}(\text{bpy})_2(4\text{-methacryloylmethyl-4}'\text{-methylbpy})]^{2+}(\text{PF}_6^-)_2$  monomer.

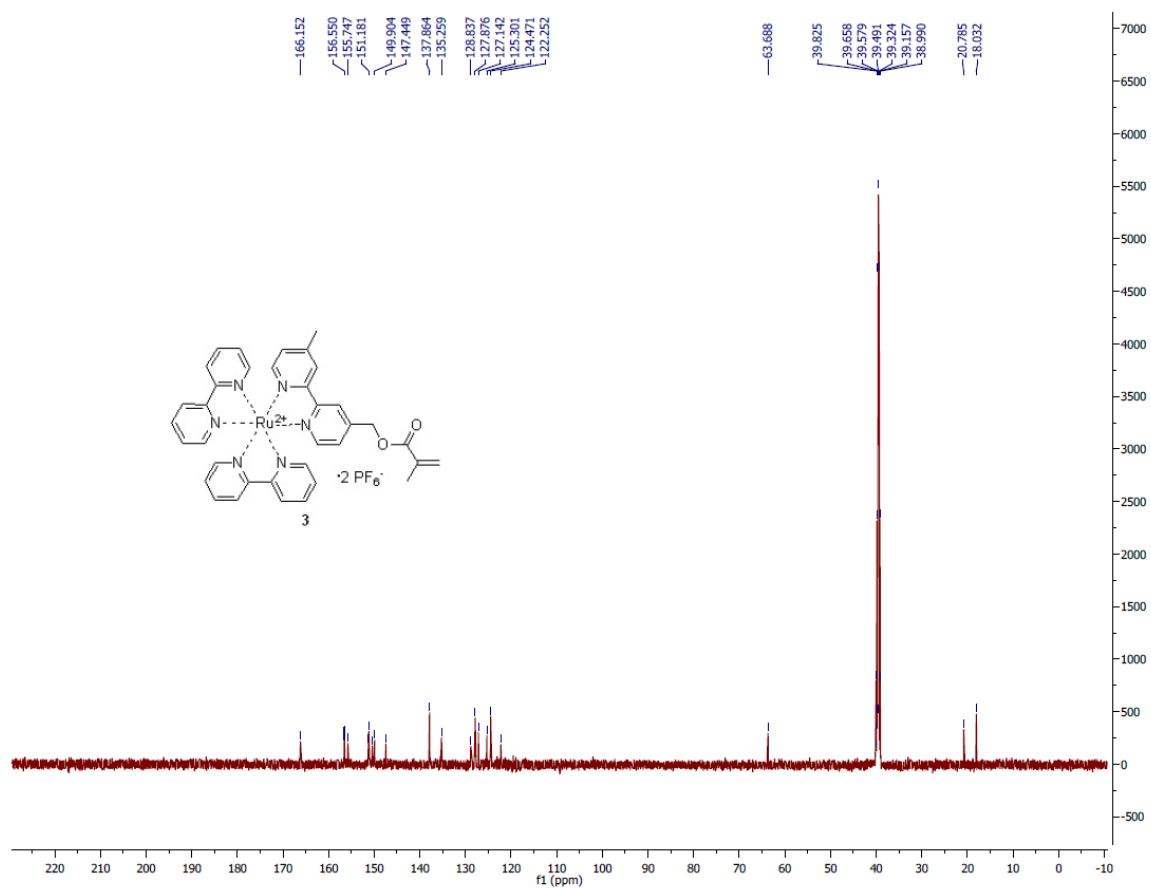
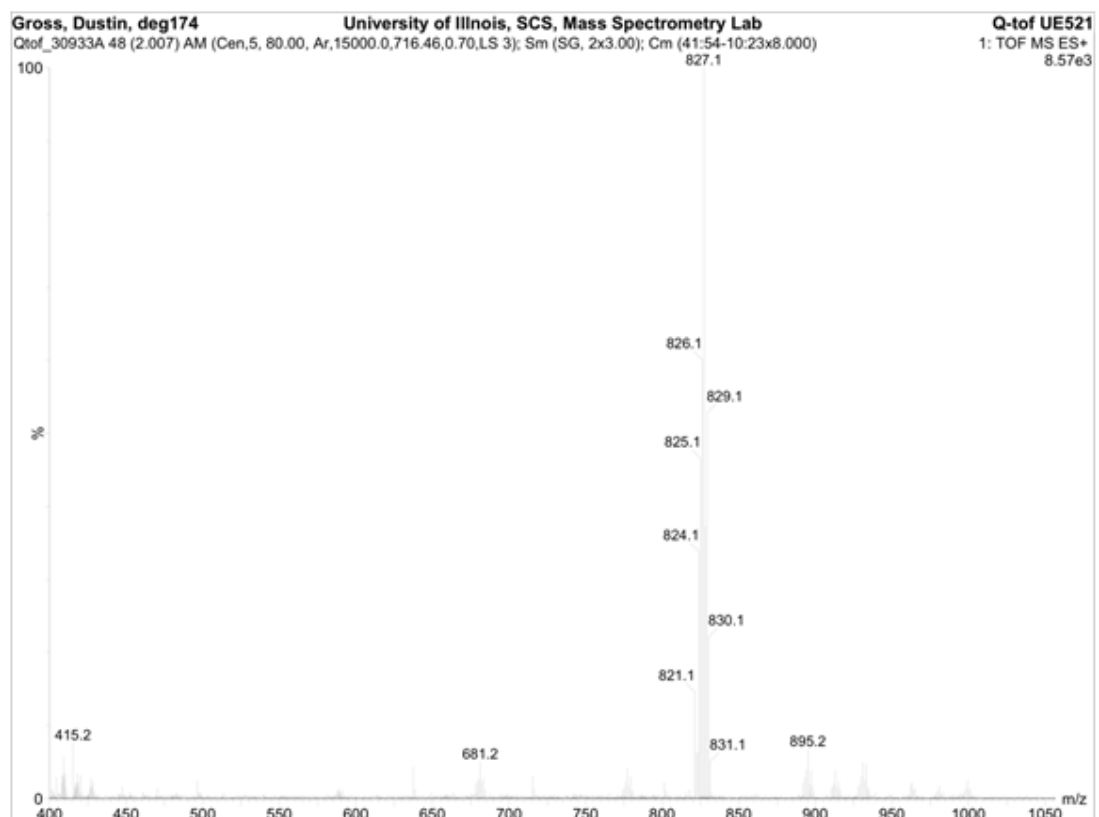


**Figure S2:**  $^{13}\text{C}$  NMR spectroscopy for  $[\text{Ru}(\text{bpy})_2(4\text{-methacryloylmethyl-4}'\text{-methylbpy})]^{2+}(\text{PF}_6^-)_2$  monomer.



Elemental Composition Report

Page 1

Single Mass Analysis

Tolerance = 10.0 PPM / DBE: min = -1.5, max = 150.0  
Element prediction: Off  
Number of isotope peaks used for i-FIT = 3

Monoisotopic Mass, Even Electron Ions

89 formula(e) evaluated with 1 results within limits (all results (up to 1000) for each mass)

Elements Used:

C: 0-120 H: 0-250 N: 5-6 O: 0-2 F: 6-6 P: 1-1 Ru: 0-1

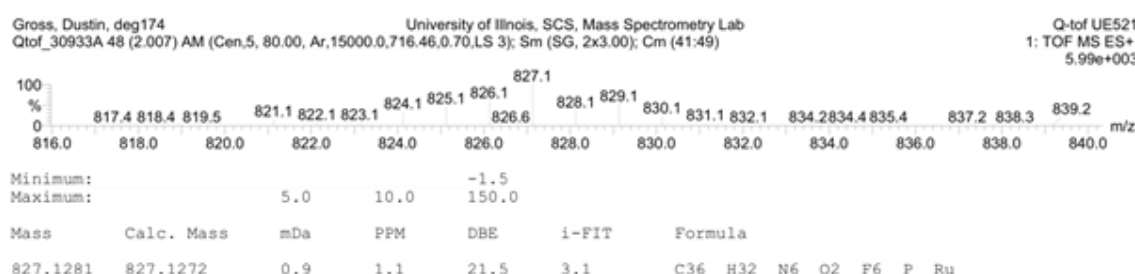


**Figure S3:** Low and High Resolution Mass Spectrometry Data for  $[\text{Ru}(\text{bpy})_2(4\text{-methacryloylmethyl-4'}\text{-methylbpy})]^{2+}(\text{PF}_6^-)_2$  monomer.

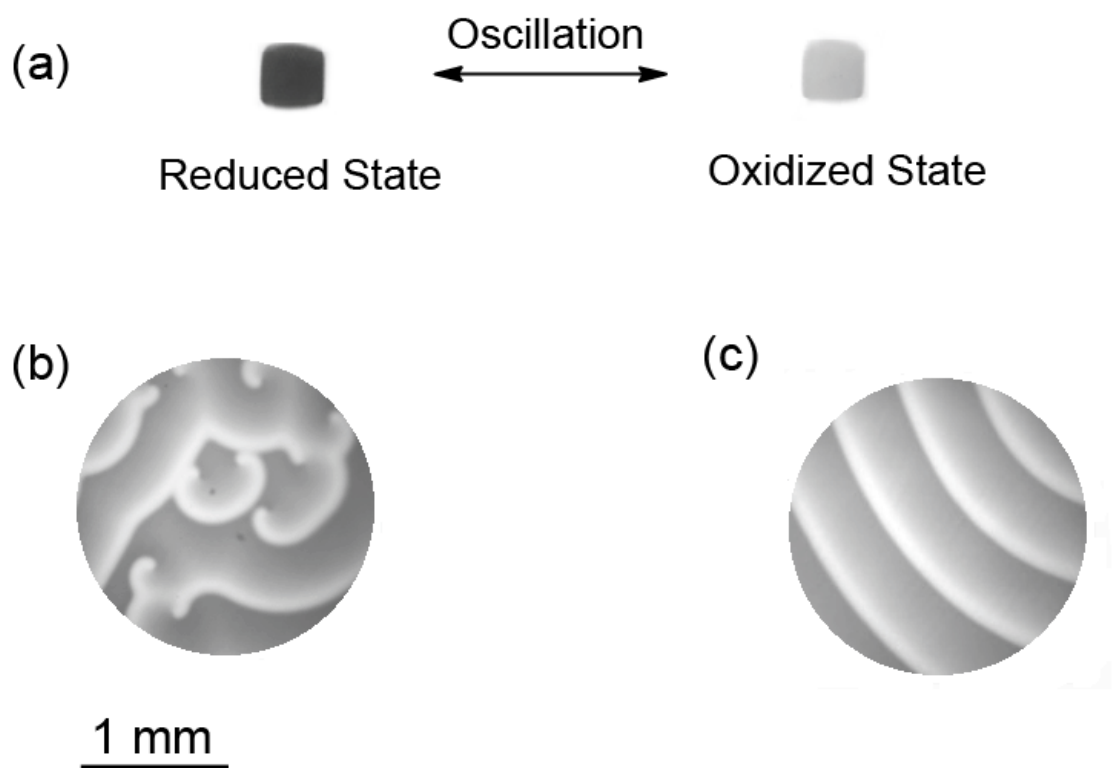


**Figure S4:** The relationship of between the size of the gel and chemical wave patterns: (a) particle size  $0.3 \times 0.3 \times 0.02$  mm, with no chemical wave patterns but simple oscillation. (b) particles size  $5 \times 5 \times 0.02$  mm, snap shot (diameter = 2mm) of the center of the particle with random patterns. (c) particles size  $5 \times 5 \times 0.02$  mm, snap shot (diameter = 2mm) of the center of the particle with regular patterns.

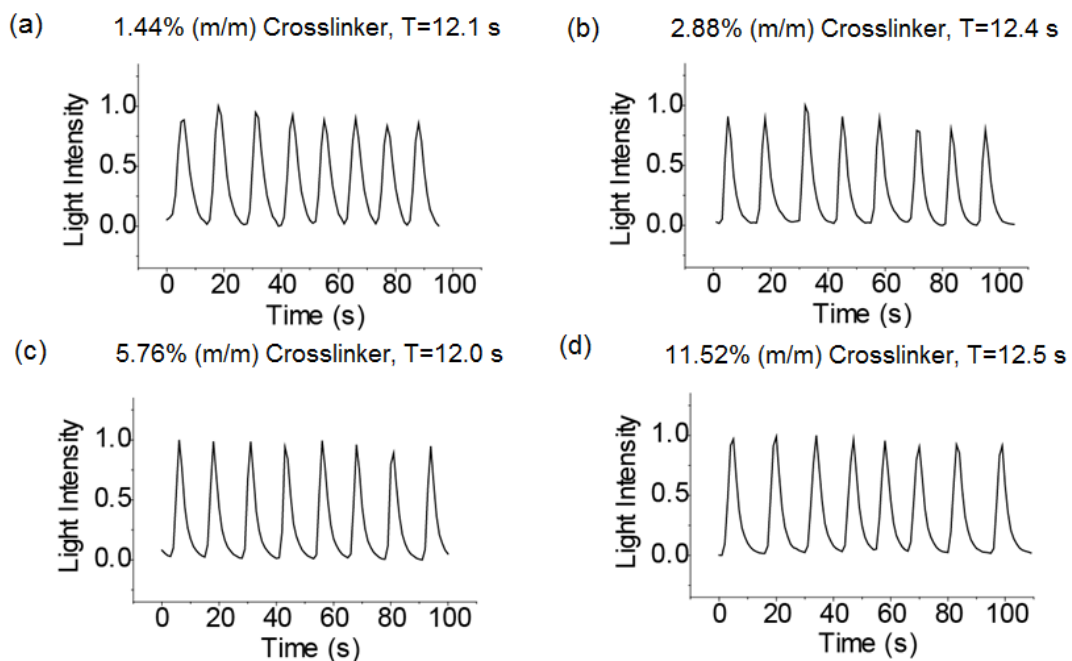


**Figure S5:** The period change of the oscillating of the gels (dimensions  $2.0 \times 0.65 \times 0.02$  mm) having different amount of crosslinkers.

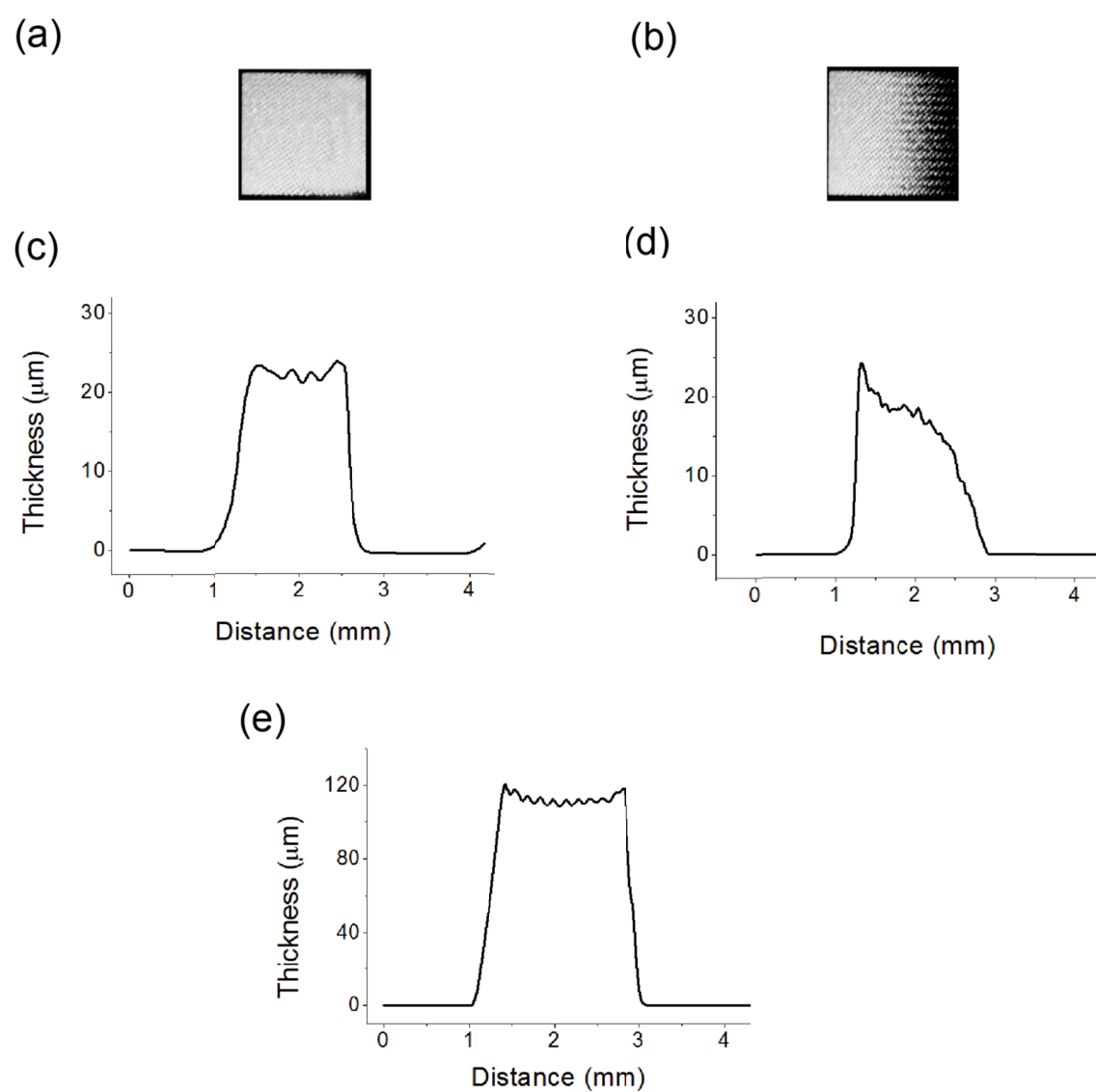


**Figure S6:** (a) the transparency of uniform darkness; (b) the transparency with gradient darkness; (c) the thickness of the gel exposed under uniform transparency; (d) the thickness of the gel exposed under gradient transparency; (e) the thickness of the gel with thicker feature.

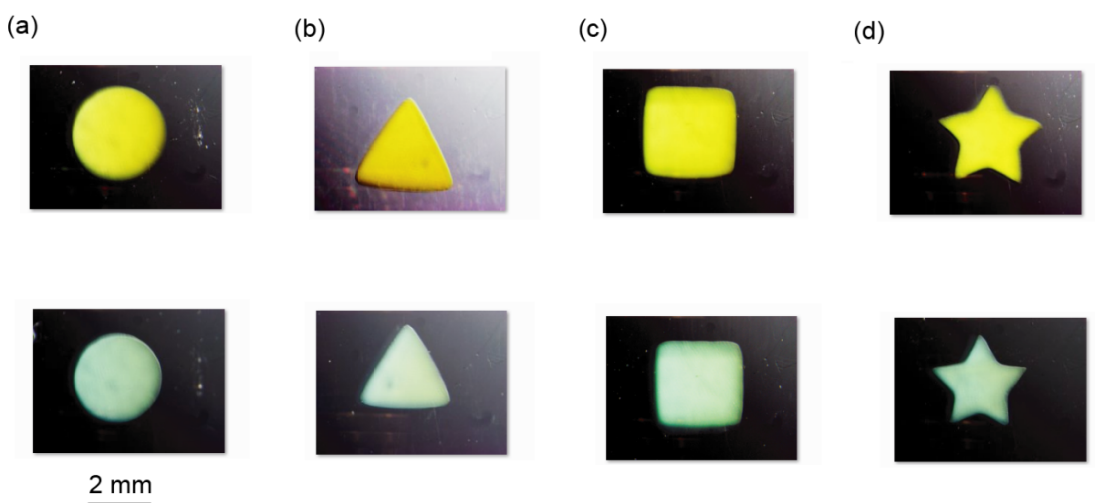


**Figure S7:** The swell-deswell properties of the methacrylate modified BZ gels: (a-d) are shape of circle, triangle, square and star respectively. The first row is reduced state ( $\text{Ru}^{2+}$ ), which is observed in  $[\text{HNO}_3]=0.5$  M solution and the second row is oxidized state ( $\text{Ru}^{3+}$ ), which is observed in solution mixture of  $[\text{NaBrO}_3]=0.20$  M and  $[\text{HNO}_3]=0.30$  M.

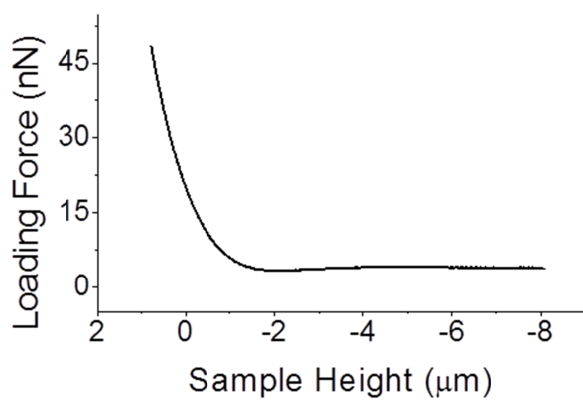


**Figure S8:** Force curve of the PAAm based self-oscillating gel, has 5.76% m/m crosslinking agent.

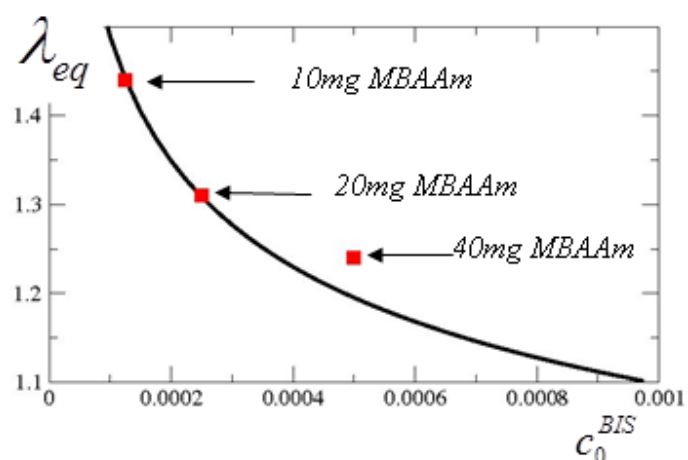


**Figure S9:** Equilibrium degree of swelling,  $\lambda_{eq}$ , as a function of the density of permanent crosslinks,  $c_0^{BIS}$ . Here, all the Ru catalyst is in the reduced state so that no additional crosslinks are formed. Red squares represent experimental data obtained for samples with 10mg, 20mg, and 40mg of MBAAm crosslinker, respectively.

#### Caption for Movie I:

**Movie I:** The propagation of chemical wave pattern and strain change due to propagating waves in the PAAm based BZ gel slab (dimensions  $2.0 \times 0.65 \times 0.02$  mm). The movie is played in real time, and it takes about 20 seconds for the chemical wave to travel through one wavelength.